Index Finger of a Human-Like Robotic Hand Using Thin Soft Muscles

Ahmad Athif Mohd Faudzi, *Member, IEEE*, Junichiro Ooga, Tatsuhiko Goto, Masashi Takeichi,
and Koichi Suzumori, *Member, IEEE*

Abstract—This letter presents an index finger of human-like robotics hand which intends to closely replicate the human finger in terms of bones, ligaments, muscles, extensor mechanism, tendon, and its pulley system. We fabricated the muscles of the index finger using thin multifilament McKibben muscles that consist of three intrinsic and three extrinsic muscles with diameters of 1.3 mm and 4.0 mm, respectively. We present the fabrication method of the index finger and model it based on the Landsmeer Model I, II, and III. We validated the properties of our developed finger with the Landsmeer model for extension and flexion motion. Finally, we demonstrated the capabilities of the finger using motion capture, *Tracker*, to compare sweeps of the HR-hand finger with a cadaver finger motion for normal and finger deformity condition. Having McKibben muscles as the actuator that mimics the human muscle, one can better understand the human finger function and may use it for training and for modeling the human finger disorders.

Index Terms—Biomimetics, biologically-inspired robots, hydraulic/pneumatic actuators, soft material robotics.

I. INTRODUCTION

THE hand has been a great tool for humans with the advantage of dexterous function and power to do daily activities such as turning a door knob, wearing clothes, using a screw driver and even playing musical instruments. The dexterous function of the hand also enables communication in the form of hand gestures for sign language as well as adding emotion while conveying a message while speaking. These dexterous hand motions are achieved due to biomechanics of hands and redundant mechanism of hand muscles [1]. Roboticist studying the function and application of robotic hand divided them into two main areas, Anthropomorphic Prosthetic Hands (APH) and Dexterous Robotic Hand (DRH) [2]. The contraction and extension of intrinsic and extrinsic muscles of hand make it possible for human to perform these dexterous tasks. Currently, research

on humanoid robots that imitate human drive mechanisms are vigorously carried out worldwide. Recent robotic hands that can demonstrate human levels of dexterity are very few, while most of them are task-based operations include KITECH-Hand [3] and EthoHand [4]. Zhe Xu *et al.* [5] developed a highly biomimetic anthropomorphic hand by including the extensor hood mechanism and proposed crochet joint to mimic those of humans but control the hand using 12 DC motor. ACT hand is one of the early available research with the same objective to replicate the human hand on anatomical level developed by Y. Matsuoka group [6]. The objectives of the developed hand are as experimental test bed to investigate the biomechanics and neural control of human hand movements and focus the motions for 3 main fingers including thumb, index and middle controlled by DC motor. Extensive results have been presented on anatomical study on the extensor mechanism [7] and the capability of the hand to play musical instrument [8].

McKibben-style actuators characterized by its high level functional analogy with human skeletal muscle are of interest. The actuator also has passive and natural compliance, which follows the nature of skeletal muscle. S. Kurumaya [9] used multifilament muscles as actuators for a lower limb robot while modeling, and force control of thin McKibben was presented by [10]. A number of robot hands have been developed with this type of actuator, including the work of Lee and Shimoyama [11]. They point out the importance of small diameter muscle for use in hands, and they have developed a tendon-driven hand with 3.5 mm diameter muscles. On the other hand, [12] propose the application of miniature pneumatic muscles for surgery manipulators. Currently, most of the APH that have been developed apply DC motor as it driving system, which carries most of the weight [2]. Some of the reported hands apply artificial muscles but it is difficult to mimic the function of the hand due to bigger diameter of the structure at 3.5 mm and difficult to incorporate it in the design [11]. A new challenge is not only to mimic the dexterity of the finger by the design but also to mimic other parts including the actuation to follow the biomechanics of hand.

In this letter, we present imitation of the biomechanics of hand anatomically focusing on the index finger from the design and structure of the intrinsic and extrinsic muscles of hand, to the bones, joint ligaments, tendon arrangement and the extensor hood mechanism as in Fig. 1. The human hand is comprised of a significant number of biological structures, resulting in a high complex redundant system. The obvious and important features to preserve this human link robotic hand are its degrees of freedom, its kinematics, its number of bones and muscles, and its muscle strengths, as well as the muscle's origin and insertion point. In addition, we want to preserve the hand's Musculotendon passive properties, its overall size, and its tendon routing

Fig. 1.   The Human-like robotic hand (HR-hand).

Joint on Finger	Associated Muscles and tendons	Range of joint motion [13]
Distal Interphalangeal (DIP)	Terminal Extensor (TE) Flexor Digitorium Profundus (FDP)	Extension-0° Flexion-60/70°
Proximal Interphalangeal (PIP)	Central Slip (CS) Lateral Band (LB) – Radial and ulnar Flexor Digitorium Superficialis (FDS)	Extension-0° Flexion-110°
Metacarpophalangeal (MP)	Extensor Digitorium Communis (EDC) Medial Band (MB) Extensor Indicis (EI) Dorsal Interossei (DI) Palmar Interossei (PI) Lumbrical (LUM)	Extension-45° Flexion-90° Ulnar deviation 30°* Radial deviation 20°*

*Average range-of-motion values of ulnar/radial deviation are usually calculated from wrist

structure. Therefore, the focus of this work is to mimic the structures of human hand according to medical literature to attain motion that is equivalent to that of the human hand. We select the bone model like human hand size and preserve its biological structure in our proposed HR-Hand. The detailed anatomy structures of bones, ligaments, muscles and finger structure are firstly identified and these are subsequently mimicked using McKibben artificial muscles and other materials.

In this initial work, we model the index finger using Landsmeer Model 1, II and III to validate the developed HR-Hand index finger. We also replicate imbalanced or malfunctioning intrinsic muscles of the fingers that could disrupt the delicate and complex balance of intrinsic and extrinsic muscles. By incorporating the biomechanical features of the hand in the HR-Hand, we intend to gvalidate the similarity properties shown by the model comparison and apply finger motion on the relation of the intrinsic and extrinsic muscles. We hope it is suitable to serve as a research apparatus to investigate human dexterity.

The remainder of the letter is organized as follows. In Section II, the index finger muscle arrangement and biomechanics model using Landsmeer model is presented. In Section III, the soft thin actuator characteristics that will represent the muscles structure are explained. Section IV discusses the methods to develop the HR-hand index finger with details on the manufacturing process. Section V shows the model validation and normal sweep and claw deformity between HR-hand and a cadaver. Section VI concludes the letter with a brief appraisal and future recommendation.

II. INDEX FINGER MODEL OF HR-HAND

A. Muscles and Joint of Index Finger

As a first step towards an entire hand, we are currently developing a complete index finger, which has all associated muscles. There are seven muscles which actively control the index finger while other fingers mainly have six muscles. The additional Extensor Indicis (EI) for index finger could perform independent extensor motion from separate muscle of Extensor Digitorium Communis (EDC). However, as it performs the same function as EDC for extension of the finger, we neglect EI and only consider EDC to be used for the finger extension. Therefore, from six, three are extrinsic muscles and three are intrinsic muscles. The extrinsic muscles are EDC, Flexor Digitorium Superficialis (FDS) and Flexor Digitorium Profundus (FDP), which are the primary movers of the MP joint for flexion-extension axis. The intrinsics include Dorsal Interossei (DI), also known as Radial Interossei, and Palmar Interossei, also known as Ulnar Interossei (UI) and Lumbrical (LUM), which act in the radial-ulnar plane about an abduction-adduction axis and contribute to Metacarpophalangeal (MP) flexion. There are 3

joints associated with the fingers which are MCP, Proximal Interphalangeal (PIP) and Distal Interphalangeal (DIP) joints. The PIP and DIP joints are considered as hinge joint for extension and flexion function while MP joint is a saddle joint that can give both motion of flexion-extension and abduction-adduction. For MP joint, the contraction of EDC will perform extension function. On the other hand, the flexor motion for all MP, PIP and DIP applies redundant mechanism of several muscles, such as the FDP, FDS, LUM, PI and DI. The muscles joint at each joint with their range of motion (ROM) are tabulated in Table I. For independent index finger, abduction (radial deviation) and adduction (ulnar deviation) of MCP joint are not usually measured. This is due to no standardized technique to measure single finger abduction and adduction in exact means. However, all finger motion of abduction and adduction form the wrist joints was reported in [13]. Therefore, we had conducted the index finger experimental evaluation and compared it with human ulnar and radial deviation in our initial work [14].

B. Biomechanics Model of Index Finger

Models of the hand are important in biomedical, reconstructive surgery and robotic fields to predict the muscle and tendon forces used while doing manipulation postures and grip function. S. Shirafuji had developed a tendon driven robotics finger that includes the lumbrical muscles in its anthropomorphic hand [15]. Tendon excursion and moment arm of index finger were studied by K.N. An *et al.* using seven hand specimens [16]. They refer to Landsmeer model [17] for the relation between excursion and joint angle.

In this work, two-dimensional models as proposed by Landsmeer (Model I, II and III) were used to compare with the results produced by the developed HR-Hand. HR-Hand could have the same properties and could mimic the function of real human hand. In this letter, the model of index finger is focused on validating flexion-extension motion only. For model simplification, we consider two main muscles of FDP and FDS for the flexion motion and EDC for the extension motion. Fig. 2 presents the schematic structure for the index finger model development.
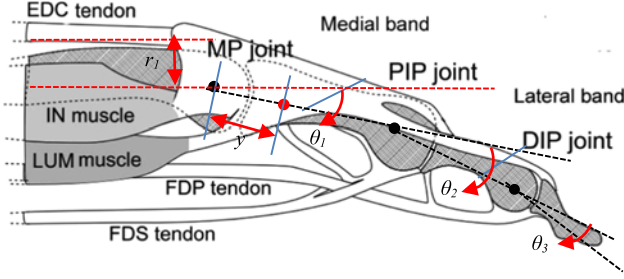
Fig. 2. Kinematic presentation of index finger.

1) Model I define the situation of tendons that track the curvature of the articular surface, which means the tendon is closely attached to the bone surface of the finger. This model is particularly designed for the extensors muscle, EDC [18] as shown in (1)

$$x_{\text{ext}} = r_1 \theta_1 \tag{1}$$

where x_{ext} is the excursion (displacement) of the extension, r_1 is the distance from the joint centre to the tendon constraint and θ_1 is the angle at the joint.

2) Model II mentioned that the system is assumed to be free of friction and the tendon runs through a loop that is freely movable around the axis. Therefore, the two parts of the tendon run parallel to the long axis of the bone and then the sling will take up a position along the bisection of the joint angle [16]. This model mostly describes the characteristics of the intrinsic muscle system. The model is shown in (2)

$$x_{\text{ext}} = 2r_1 \sin\left(\frac{\theta_1}{2}\right) \tag{2}$$

where x_{ext}, r_1 and θ_1 are similar to (1).

During our experiment, we try to apply Model II for extension motion to validate it with Model I.

3) In Model III, it considers the tendon runs in a tendon sheath that holds it firmly in a constant position against the shaft of the bone, but allows the tendon to curve smoothly in the joint angle for minor bowstring. This occurs because the annular pulley is located on the bottom of the volar plate. The model is shown in (3) for both extension and flexion

$$x_{\text{ext}} = \theta_1 d_1 + r_1\left(2 - \frac{\theta_1}{\tan(\frac{\theta_1}{2})}\right) \tag{3}$$

$$x_{\text{FDP}} = \theta_1 d_1 + r_1\left(2 - \frac{\theta_1}{\tan(\frac{\theta_1}{2})}\right) + \theta_2 d_2$$

$$+ r_2\left(2 - \frac{\theta_2}{\tan(\frac{\theta_1}{2})}\right)$$

$$+ \theta_3 d_3 + r_3\left(2 - \frac{\theta_3}{\tan(\frac{\theta_3}{2})}\right) \tag{4}$$

$$x_{\text{FDS}} = \theta_1 d_1 + r_1\left(2 - \frac{\theta_1}{\tan(\frac{\theta_1}{2})}\right) + \theta_2 d_2$$

$$+ r_2\left(2 - \frac{\theta_2}{\tan(\frac{\theta_2}{2})}\right) \tag{5}$$

where x_{ext}, $x_{\text{FDP}}, x_{\text{FDS}}$ are the tendon displacement past the joint, θ_1, θ_2, θ_3 are the joints at each finger joint and d_1, d_2, d_3 are the distance along the axis of bone from the point where the tendon begins to curve to joint center. Model III is normally applied for finger flexion. However, we also applied model III for finger extension motion for validation purpose.

III. THIN SOFT MCKIBBEN MUSCLES

A. Thin Soft McKibben Actuator

We developed thin McKibben muscles [19] that resemble biological muscles with contraction ratio similar to some vertebrae muscle, which usually shortens by 25% or less. The soft actuators offer an attractive performance in various aspects including robustness, simplicity, high specific force to weight ratio for a given input pressure [20]. These characteristics make it very attractive for a wide range of applications such as robotic hand and prosthetic appliances for the disabled [21]. [6] reported the use of conventional actuators to closely mimic human hand structures, however it is difficult due to their relatively large size and relatively fixed designs. The usage of the developed thin and soft McKibben muscles that possess the natural compliance of the antagonistic muscular function enables the realization of robotic hand that closely mimic the human anatomy.

Two different diameters of multifilament McKibben muscles were used for HR-hand. The intrinsic muscles apply 1.3 mm outer silicone rubber tube while the extrinsic muscles apply 4.0 mm outer silicone rubber tube. Both tubes were covered by multifilament Vectran sleeves. The Vectran multifilament were woven around the silicone tube making the overall outer diameter of the actuator 1.9 mm and 4.6 mm, respectively. The fiber angle was set to 19 degrees for optimum contraction function of the actuator. The inner silicone tube has E = 1 MPa and break point of 585% from the initial position with hardness of 40 ShoreA.

B. Force Characterization and Contraction Ratio

The actuators exhibit contraction force, which is proportional with the contraction ratio. This is confirmed with force characterization experiments as shown in Fig. 3. The 4.0 mm exhibit higher force around 43 N at 0.4 MPa while the 1.3 mm, which has advantage in miniature diameter, suffer smaller contraction force of 5 N at 0.4 MPa. The 4.0 mm and McKibben actuator exhibit contraction ratio of 22% at 0.3 MPa and 25% at 0.4 MPa while the 1.3 mm muscle has a slightly higher contraction ratio compared to 4.0 mm muscle. The averaged tendon forces for different pinch and grasp configurations in the index finger intrinsic muscle were referred from [22]. Based on these values, 1.3 mm muscles is sufficient to drive the intrinsic muscles. For the extrinsic muscles, Skyler et al. [23] mentioned in their work that the amount of force needed for flexion applying FDS and FDP requires force of around 20 N. Therefore, 4.0 mm could be used for extrinsic muscle which requires higher force value. The
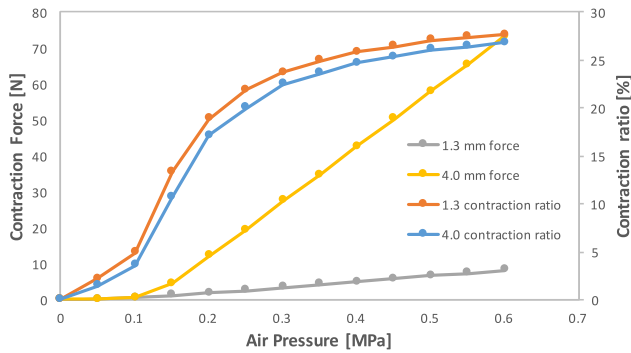
Fig. 3. Contraction force and contraction ratio during different input pressure.

TABLE II
DIMENSION OF THE INDEX FINGER SPECIMEN

Phalanx	Distal (mm)	Middle (mm)	Proximal (mm)	Metacarpal (mm)
Overall length	15	23	39	70
1	3	8	7	12
2	2	6	8	7
3	7	11	14	16

HR-Hand will be operated with input pressure ranging from 0.1 to 0.45 MPa using analog valve.

IV. FABRICATION OF HR-HAND INDEX FINGER

In this work, the objective is to attain an index finger with characteristics like the human index finger that provides an equivalent motion. Thus, the main anatomic structures of the index finger were first identified, and subsequently mimicked accordingly. The main anatomic features of bones, ligament, muscles, extensor hood mechanism and pulley system are described in Subsections IV-A, IV-B, IV-C, IV-D, IV-E respectively, together with the method to mimic them. Specific details about the manufacturing process are also included in these subsections.

A. Bones

The HR-Hand bones were mimicked using a readily available upper limb model from 3B Scientific (Hamburg, Germany), with part number A45. It consists of carpal bones, phalanges, forearms and humerus bones for the overall HR-Hand fabrication. The bone structure was made from natural cast and was molded from the actual specimen of male human adult with a height of 160 cm. It is made of resin material and has the advantage of lightweight and high strength. Surface smoothing was manually applied using *paraffin* to ensure a smooth articulation at the regions of contact between bones. There are 27 bones in the hand – eight carpals in the wrist; five metacarpals in the palm of the hand; and 14 bones in the fingers, called the proximal, middle, and distal phalanges. The lengths of each phalanges of index finger; distal, middle, proximal and metacarpal are given in Table II based on measurement conducted as in Fig. 4. Four measurement were taken for each phalanx, its length, the diameter at point 1, 2 and 3. One interesting points to note regarding the bone structure is that some of the bone bumps allow specific routing for tendon, which can assist its motion and limit
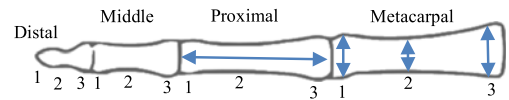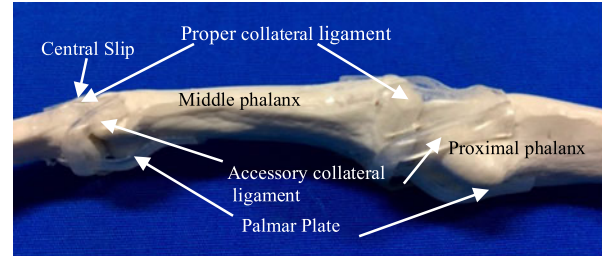

Fig. 4. Bones of index finger.

Fig. 5. Ligaments of the bone following the structural of real hand.

the movement of ROM. The size of the index finger is slightly small compared to [16].

B. Ligament

Ligaments structure are strong bands of tissue made of collagen, that connects bone to bone together and provide mobility and stability to the hand. In the finger phalanx, important ligaments are proper ligaments, accessory collateral ligaments and palmar plate (volar ligaments). There are few other ligaments related to extensor mechanism that will be covered in Section IV-D. All ligaments were mimicked in this work. The ligaments were imitated by using hyperelastic materials from silicone of the soft McKibben muscles. The property of the silicone was presented in Section III-A. The thickness of 1 mm is suitable to reproduce the ligament geometry to attain a similar stiffness to that of the human equivalents.

Fig. 5 shows the structure of ligaments around the MP joints and which were fabricated between proximal phalanx, middle and distal phalanx. We use Loctite 401TM (Dusseldorf, Germany) to fix the silicon to the bone. As the silicone can follow the contour of the bone, process of fixing is easy. We fabricate the ligaments following the actual joint architecture of the humans. The collateral ligaments arise from the side of the metacarpal head and pass obliquely downwards to insert into the phalanx, thereby maintain the finger motion during finger flexion and extension. The palmar plate helped to control the finger motion by loose in flexion and tight during extension to prevent hyperextension. This method reduces the complexity like other finger joint design using crochet [27] and gimbal [28] while keeping the similar range of motion (ROM) of the joint as tabulated in Table I. We conducted lateral pulling test to identify the connecting strength between the silicone and the bone structure. The silicone connection could support lateral force till 10.5 N which is sufficient for the HR finger design.

C. Muscles

The index finger comprises of two main muscles of intrinsic and extrinsic. The intrinsic muscles are muscles characterized by the origin and insertion in the palm of the hand while for extrinsic muscles the origin is mainly from the forearm. In this subsection, we will present the process of fabricating of both intrinsic and extrinsic muscles.
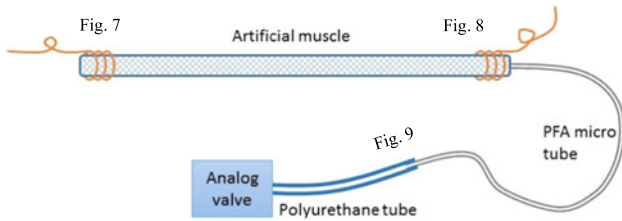
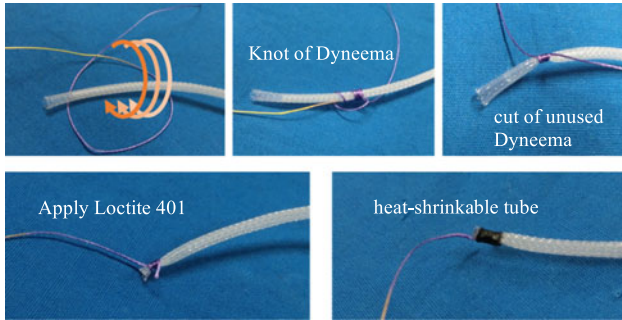Fig. 6.   Structure of the 1.3 mm McKibben muscle.
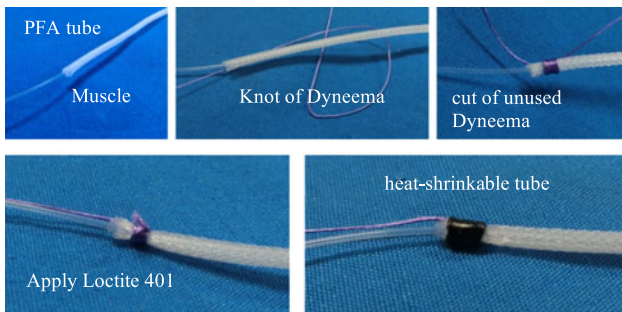

Fig. 7.   Fabrication of end part of 1.3 mm actuator.

Fig. 8.   Fabrication of end part of 1.3 mm actuator (to air supply).

1) Intrinsic Muscles: The intrinsic muscles for the index finger, LUM, DI and PI use 1.3 mm soft McKibben muscles. The small diameter makes it possible to mimic the exact origin and insertion position of the muscle. For the index finger, DI is originated from the left side (radial side) of the metacarpals with bipennate muscles while inserted at two points, extensor expansions and bases of proximal phalanges. On the other hand, PI is originated from the right side (ulnar side) of the metacarpals with unipennate muscles while inserted at the extensor expansion. The LUM has unique origin and insertion where it originates from FDP muscle and inserts at the Radial lateral band of the extensor expansion (tendon) dorsal aponeurosis. Although the LUM produce less force compared to PI and DI, it is one of the main extensors of the interphalangeal joints. Most of the robotic fingers could not incorporate this muscle because of the fabrication problem.

The structure of the 1.3 mm artificial muscle is shown in Fig. 6. Details of each part will be described below in Figs. 7, 8 and 9. After finishing the fabrication process, all muscles will be placed at the origin and the insertion point referring to the actual human hand muscle anatomy [24], [25]. The first end part is sealed by making a knot using a Dyneema (high-density polyethylene) fishing line, manufactured by Daiwa. Co., Ltd. (Japan) with part number PE-4. Since load is applied to the
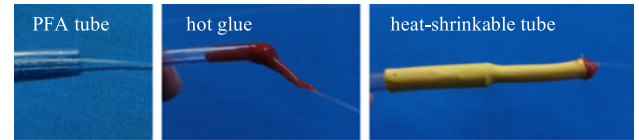

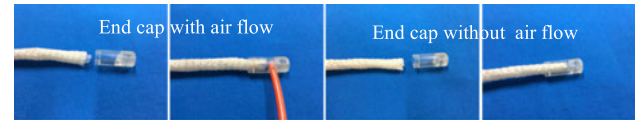Fig. 9.   Connection of PFA tube to 4 mm polyurethane tube.

Fig. 10.   Fabrication of both end part of 4.0 mm actuator.

Dyneema, we applied inner latch knot as in Fig. 7 for strong bond between Dyneema and the muscle. The Dyneema is pulled strongly and the Dyneema on the side wrapped around the artificial muscle is cut. After cutting, Loctite 401 (Dusseldorf, Germany) was adhesive to the knot and covered by a heat-shrinkable tube SUMITUBE W3F2, manufactured by Sumitomo Electric Industries Inc. (Osaka, Japan). On the other end of the actuator, air tube, Exlon-PFA (0.6x 0.4 mm) with part number 5F1Y13 manufactured by Iwase Co. Ltd (Kanagawa, Japan) was used to supply air input to the actuator. As the air supply tube is thin, the required length of air tube is initially cut and inserted inside the McKibben muscle it for 15 mm as in Fig. 8. Then, lightly tie the same knot of Dyneema as above before cutting the unused part. However, if the Dyneema was tighten too strong it will restrict the air flow to the actuator. Loctite 401 was applied to the knot and covered with the SUMITUBE W3F2 heat-shrinkable tube. In order to connect the PFA tube to the analog valve, a polyurethane air tube with outside diameter of 4 mm is needed. Again the PFA tube is inserted inside the polyurethane tube and sealed using hot glue, HB-40S-1K from Taiyo Electric Ind. Co., Ltd. (Fukuyama, Japan) about 30 mm from the mouth of the tube. SUMITUBE W3F2 heat-shrinkable tube is once again applied to hold the joints together and secure for leakage as in Fig. 8.

2) Extrinsic Muscles: The muscles used for activating index finger flexion motion are the extrinsic muscle of FDP and FDS. On the extension side, EDC extends the digit with the help of the extensor mechanism structure. All extrinsic muscles were fabricated using 4.0 mm McKibben muscles as in Fig. 10. Each end of the actuator is sealed with 3D printed end cap using Keyence Agilista 3200 3D printer. One of the two end cap has a small hole for air flow inside the actuator using 3 mm polyurethane tube. Loctite 401 was applied to seal from air leakage.

3) Selection of Muscles Length: The selection method of actuator length for intrinsic muscle and extrinsic muscles are slightly different. For all intrinsic muscles, the length of the muscles were based on the actual placement of origin and insertion point [24], [25]. On the other hand, the length of the actuator for extrinsic muscles depends on the ROM of flexion and extension of the finger motion [14] and excursion data actual muscle [18]. Based on the characteristics experiment of the actuator conducted in [19], it shows that the contraction ratio and force are the same at any length of the actuator. The contraction ratio only changes at different pressure input e. g. 18.5% and 24% at 0.3 MPa and 0.35 MPa respectively. The length of all muscles for index finger are tabulated in Table III.

TABLE III
LENGTHS OF MUSCLES FOR INDEX FINGER

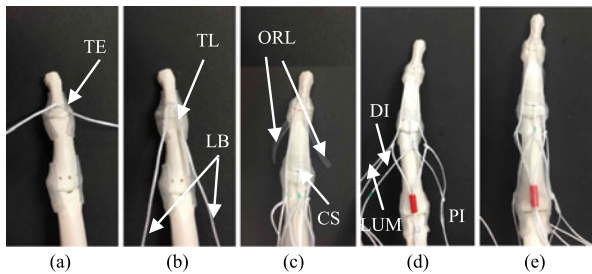| Muscles	Initial length of actuator	Contracted length at 0.3 MPa	Contracted length at 0.4 MPa
EDC	125 mm	25 mm	28.8 mm
FDP	175 mm	35 mm	40.3 mm
FDS	150 mm	30 mm	34.5 mm
LUM	50 mm	10 mm	16 mm
PI	54 mm	11 mm	13 mm
DI	59 mm	12 mm	14 mm

Fig. 11. Fabrication of extensor mechanism. (a) Dyneema is fixed at base of distal phalanx as TE. (b) TE was fixed with 0.3 mm ligament to form TL. (c) ORL was fixed from LB to the middle phalanx; CS was fixed at base of middle phalanx using Dyneema. (d) Distal wing was formed from CS for LUM, PI and DI. (e) SB, OF, TF, RL ligaments were fixed to complete the extensor mechanism structure.

D. Extensor Mechanism

The extensor mechanism, also known as dorsal aponeurosis, has a unique web structure that makes it possible to assist in the control finger motion. In the past, this structure had been neglected in most anthropomorphic robotic hand due to its complex structure [7]. We identified that this extensor mechanism gives independent control of the MP joint and acts not only as an extensor but also as a flexor, abductor, adductor, or rotator depending on the finger's posture. We used additional silicone rubber sheet As-One Co. Ltd (Osaka, Japan) (part number 6-611-01) with 0.3 mm thickness for fine ligaments on the extensor mechanism. Examples of ligaments fabricated using the silicone rubber are Sagittal Band (SB), Oblique fibers (OF), Transverse fibers (TF), Retinacular ligaments (RL), Oblique Retinacular Ligament (ORL) and Triangular Ligament (TL) [26]. We applied Dyneema (high-density polyethylene), manufactured by Hayama Ind. Co., Ltd. (Nagahama, Japan) with part number DB-8HE, with 0.53 mm diameter as tendon and as extensor mechanism web. The tensile strength is 489.92 N with percentage of elongation of 4.09%. Fig. 11 shows the step by step fabrication process of the extensor mechanism. The lateral band (from ulnar band and radial band) is formed as a single attachment to the dorsal side of the distal phalanx as Terminal Extensor (TE) to transmit force from the EDC, LUM, PI and DI. The lateral band and the extensor hood play a big role in the manipulation of finger. The first function of lateral band is to assist the abduction and adduction from the interossei muscles (PI and DI). Second, it allows extension of the distal phalanx and the whole finger with activation of EDC muscle. Finally, it coordinates the DIP and PIP in flexion and extension to ease in pinching function with the help of LUM muscles. The normal sweep of flexion of hand is assisted by the interossei and LUM muscle that help to extend the PIP while flexing the MP. This
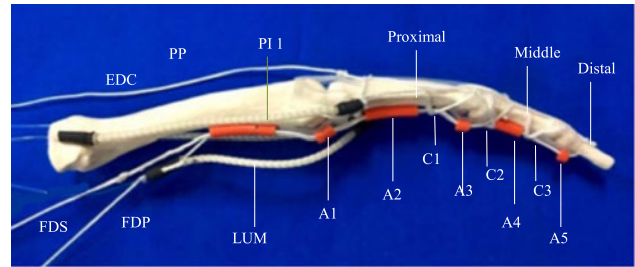

Fig. 12. Index finger pulley system.

makes it possible for us to grab bigger objects than our hand, for example a basketball.

E. Tendon and Pulley System

We refer the anatomy of the flexor tendon sheaths and pulley system as in [27]. Tendon for all extrinsic muscles uses Dyneema DB-8HE with 0.53 mm diameter. The high tensile strength makes it suitable to be used and connect to the muscles. These tendons are surrounded and enclosed by the synovial sheaths fabricated using 3.0 mm polyethylene tube. We mimic and fabricate all pulley systems as in Fig. 12. Among all pulleys, A2 and A4 are the most important pulleys at the proximal and middle phalanx with hard structure that holds down the tendon to the bone to prevent bowstringing. Major bowstring would cause rupture of the A2 and A4 pulley. The pulley advancement increased the tendon excursion required to flex the joint, and thus giving the mechanical advantage of this joint [16]. A1, A3, and A5 that overlie the MP, PIP and DIP joints, respectively, originate from each joint palmar plate. The cruciate pulleys C1, C2 and C3 prevent sheath collapse and expansion during finger motion and facilitates annular pulleys during flexion.

V. EXPERIMENTAL EVALUATION AND DISCUSSION

We conducted two studies to validate the developed HR-Hand index finger. The first method is to compare the index finger flexion-extension motion with the Landsmeer Model I, II and III. The second method is to apply normal flexion sweep and claw deformity, a condition where the function of all intrinsic muscles is impaired.

A. Comparison Between Landsmeer Model I, II and III

The Landsmeer Model presented in Section II was compared with the experimental evaluation for extension and flexion motion. Fig. 13(a) shows the extension motion of the EDC muscle from $-30°$ (initial position of the finger) to $45°$ with the excursion of the tendons and compared to the three Landsmeer models I, II and III at MP joint. Comparing the experiment to the models, Model I gives the smallest error followed by Model II and Model III which agrees with the theories where Model I is the most suitable equation for extension. Maximum excursion for extension is around 15 mm.

We further validated the experiment with flexion motion and used only Model III as it is suitable to adapt the bowstring condition that occurs on the volar side of the finger from initial point to $90°$ of flexion. We performed model comparison in time based as to show the time required to perform complete flexion around 50 ms. Fig. 13(b) shows similar properties between experimental and calculated excursion with errors of less
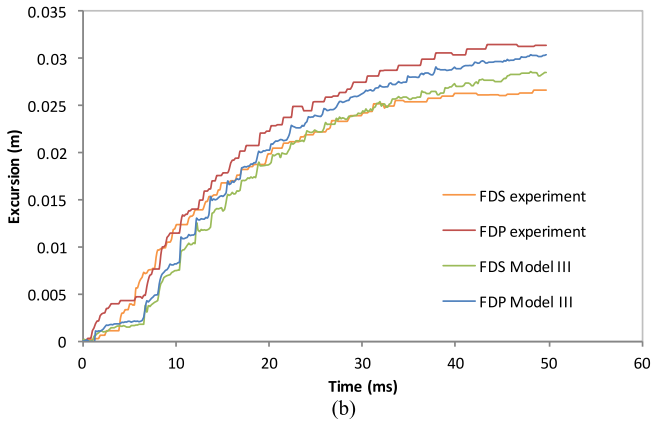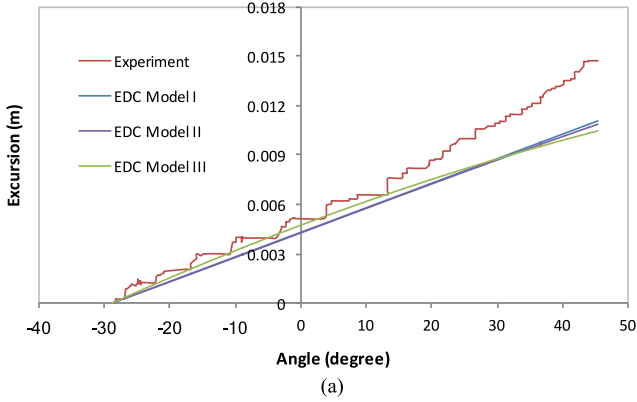
Fig. 13.   (a) Extension motion using EDC muscle. (b) Flexion motion using FDS and FDP.
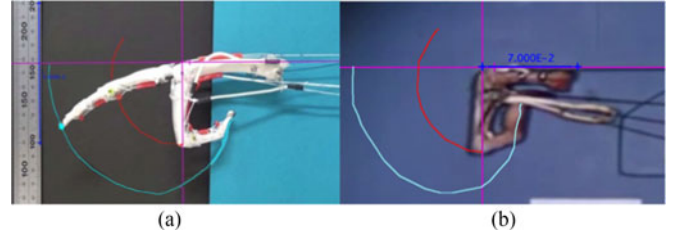

Fig. 14.   Comparison of normal sweep and claw deformity for (a) HR-Hand and (b) cadaver model.

Fig. 15.   Experiment and cadaver motion for normal sweep and claw deformity.

than 10% for both FDS and FDP. Values of excursion of EDC, FDP and FDS were also compared with [16]. As size of the bones is slightly different, and actual human muscle are fully optimized, the experimental excursion gives more to displacement to achieve complete $90°$ flexion of 20 mm and 30 mm respectively. The similar angle flexion in [16] of FDP and FDS reported only requires 20 mm to achieve complete flexion.

B.   Normal Sweeps and Claw Deformity of Index Finger

The loss of muscle function primarily affects IP joints but also may affect MP joints. The condition, which allows the hand to be so versatile and functional, is by applying both intrinsic and extrinsic muscles in its proper extension and flexion motion. Here, we conduct an experiment to identify the roles of PI and DI for flexion motion by testing two modes of hand condition 1) normal flexion sweep applying all extrinsic and intrinsic, 2) a claw deformity flexion applying only extrinsic muscles due to disrupted and malfunctioning intrinsic muscles as in Fig. 14. Both conditions will be compared with a cadaver experiment [28] using motion capture analysis. Feedback data are recorded using data logger and video camera image. Later, the captured data were analyzed by using *Tracker*, an open source motion capture analysis tool. The mapping of both HR-Hand and the cadaver were plotted in Fig. 15 tracking the fingertip motion of normal sweep and claw deformity condition. The graph shows the index finger flexion motion at MP joint from $15°$ extension angle until full flexion of $90°$. The pressure reading of all muscles for both properties were shown in Fig. 16.
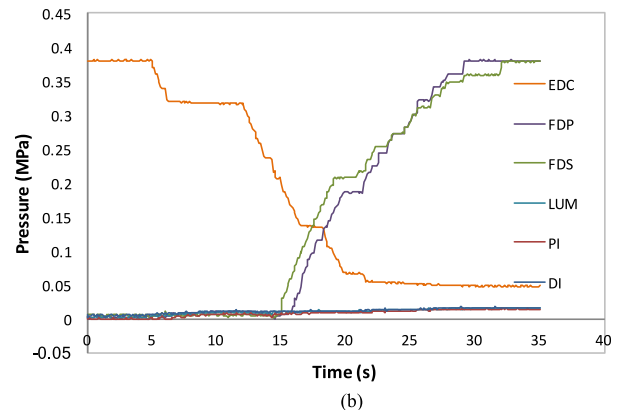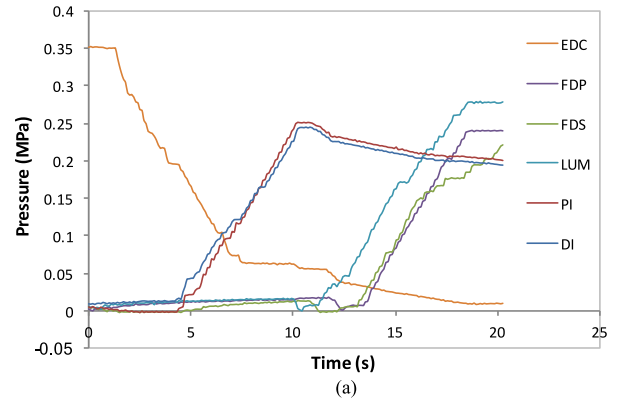

Fig. 16.   (a) Pressure reading for the muscles during normal sweep. (b) Pressure reading for muscles during claw deformity.

The finger was first tested with normal sweep by applying all 6 muscles of the finger intrinsic (LUM, PI, DI) and extrinsic (EDC, FDP and FDS). Then, claw deformity property was performed by only applying the extrinsic muscles.

From the Fig. 16(a), we identify that from $t = 5$ s to 10 s, both PI and DI were activated to assist for normal sweep of the hand flexion. Both PI and DI muscles extend the PIP joint while flexing the MP joint making the flexion motion moves smoother. The flexion motion is completed with the activation of FDP and FDS muscles to obtain maximum grip (complete flexion). In the case of direct activation of FDS and FDP directly after activation of EDC in Fig. 16(b) the finger will exhibit claw deformity, which reduces the range of motion of the finger flexion. The data shows that the HR-Hand could map the similar motion with the cadaver motion for both normal sweep and claw deformity showing biomechanical properties of the developed hand. The interossei of intrinsic muscles plays important role for flexing the MP joint while extending the PIP and DIP joint. The function of LUM also helped in obtaining the full flexion by pulling the MP joint.

VI. CONCLUSION AND FUTURE WORK

In this letter, a new "HR-Hand" applying thin McKibben actuators as intrinsic and extrinsic muscles was presented focusing on the index finger. Other biomechanic properties of hand including bone, joint ligaments and tendon arrangement, pulley and extensor mechanism were also applied with detailed fabrication methods. The experiment evaluation of tendon excursion and angle of the index finger shows our validation of the finger is as the Landsmeer Model. The performed experiment on normal flexion sweep and claw deformity also shows that the finger could develop the similar deformity and could be used to further study any condition of hand by manipulating the muscle activity. We also observed the redundant muscles strategy and understand each muscle functions that affects the motion of fingers. This shows how non-clinicians can also understand the human-hand mechanisms without access to cadaver and use HR-Hand as an apparatus to learn hand muscles. As an extension to the work, it would be interesting to assess on closed loop control and optimization of its motion mapping. Completion of the HR-Hand makes it possible for actual human hand properties to be used in robotics in the future.

REFERENCES

[1] A. Bicchi, "Hands for dexterous manipulation and robust grasping : A difficult road toward simplicity," *IEEE Trans. Robot. Autom.*, vol. 16, no. 6, pp. 652–662, Dec. 2000.

[2] H. Liu, D. Yang, S. Fan, and H. Cai, "On the development of intrinsically actuated, multisensory dexterous robotic hands," *ROBOMECH J.*, vol. 3, no. 4, pp. 1–9, 2016.

[3] D. Lee, J. Park, S. Park, M. Baeg, and J. Bae, "KITECH-hand : A highly dexterous and modularized robotic hand," *IEEE/ASME Trans. Mechatronics*, vol. 22, no. 2, pp. 876–887, Apr. 2016.

[4] C. Konnaris, C. Gavriel, A. A. C. Thomik, A. A. Faisal, and M. Ieee, "EthoHand thoHdexterous robotic hand with ball-joint thumb enables complex in-hand object manipulation," in *Proc. IEEE Int. Conf. Biomed. Robot. Biomechatronics*, 2016, pp. 1154–1159.

[5] Z. Xu and E. Todorov, "Design of a highly biomimetic anthropomorphic robotic hand towards artificial limb regeneration," in *Proc. IEEE Int. Conf. Robot. Autom.*, 2016, pp. 3485–3492.

[6] A. D. Deshpande *et al.*, "Mechanisms of the anatomically correct testbed (ACT) hand," *IEEE/ASME Trans. Mechatronics*, vol. 18, no. 1, pp. 238–250, Feb. 2013.

[7] D. D. Wilkinson, M. Vande Weghe, and Y. Matsuoka, "An extensor mechanism for an anatomical robotic hand," in *Proc. IEEE Int. Conf. Robot. Autom.*, 2003, pp. 238–243.

[8] A. Zhang, M. Malhotra, and Y. Matsuoka, "Musical piano performance by the ACT hand," in *Proc. IEEE Int. Conf. Robot. Autom.*, 2011, pp. 3536–3541.

[9] S. Kurumaya, K. Suzumori, H. Nabae, and S. Wakimoto, "Musculoskeletal lower-limb robot driven by multifilament muscles," *ROBOMECH J.*, vol. 3, no. 1, p. 18, 2016.

[10] A. A. M. Faudzi, N. H. Izzuddin, and K. Suzumori, "Modeling and force control of thin soft McKibben actuator," *Int. J. Autom. Technol.*, vol. 10, no. 4, pp. 487–493, 2016.

[11] Y. K. Lee and I. Shimoyama, "A skeletal framework artificial hand actuated by pneumatic artificial muscles," in *Proc. 1999 IEEE Int. Conf. Robot. Autom.*, May 2009, vol. 2, pp. 926–931.

[12] T. Ranzani, G. Gerboni, M. Cianchetti, and A. Menciassi, "A bioinspired soft manipulator for minimally invasive surgery," *Bioinspiration Biomimetics.*, vol. 10, no. 3, 2015, Art. no. 35008.

[13] F. Dincer and G. Samut, "Physical examination of the hand," in Hand Function: A practical Guide to Assessment, pp. 23–40, 2014.

[14] A. A. M. Faudzi, K. Suzumori, O. Junichiro, and T. Goto, "Intrinsic muscles of human-like robotic hand using McKibben actuator," in *Proc. JSME Conf. Robot. Mechatronics*, 2017, pp. 2PI–L06.

[15] S. Shirafuji, S. Ikemoto, and K. Hosoda, "Development of a tendon-driven robotic finger for an anthropomorphic robotic hand," *Int. J. Robot. Res.*, vol. 33, no. 5, pp. 677–693, 2014.

[16] K. N. An, Y. Ueba, E. Y. Chao, W. P. Cooney, and R. L. Linscheid, "Tendon excursion and moment arm of index finger muscles," *J. Biomech.*, vol. 16, no. 6, pp. 419–425, 1983.

[17] J. M. Lansdmeer, "Study in the anatomy of articulation 1. The equilibrium of the 'intercalated' bone," *Acta Morphol. Neerl. Scand*, vol. 3, pp. 287–303, 1961.

[18] K. N. An, E. Y. Chao, W. P. Cooney, and R. L. Linscheid, "Normative model of human hand for biomechanical analysis," *J. Biomech.*, vol. 12, pp. 775–788, 1979.

[19] M. Takaoka, K. Suzumori, S. Wakimoto, S. Iijima, and T. Tokumiya, "Fabrication of thin mckibben artificial muscle with various design parameters and their experimental evaluations," in *Proc. 5th Int. Conf. Manuf., Mach. Des. Tribol.*, 2013, p. 82.

[20] T. Rehman, A. A. M. Faudzi, D. E. O. Dewi, K. Suzumori, M. R. M. Razif, and I. N. A. M. Nordin, "Design and analysis of bending motion in single and dual chamber bellows," *J. Teknol.*, vol. 78, nos. 6–13, pp. 17–23, 2016.

[21] I. N. A. Mohd Nordin, M. R. Muhammad Razif, A. A. M. Faudzi, E. Natarajan, K. Iwata, and K. Suzumori, "3-D finite-element analysis of fiber-reinforced soft bending actuator for finger flexion," in *Proc. IEEE/ASME Int. Conf. Adv. Intell. Mechatronics*, 2013, pp . 128–133.

[22] E. Y. Chao, J. D. Opcrande, and F. E. Axmear, "Three-dimensional force analysis of finger joints in selected isometric hand functions∗," *J. Biomech.*, vol. 9, pp. 387–396, 1976.

[23] S. A. Dalley, T. E. Wiste, T. J. Withrow, and M. Goldfarb, "Design of a multifunctional anthropomorphic prosthetic hand with extrinsic actuation," *IEEE/ASME Trans. Mechatronics*, vol. 14, no. 6, pp. 699–706, Dec. 2009.

[24] D. Moore, "Ortho bullets." [Online]. Available: http://www.orthobullets.com/anatomy/10025/flexor-carpi-ulnaris?expandLeftMenu=true

[25] M. B. Wood, "Hand intrinsic muscle reanimation by transfer of the distal portion of the anterior interosseous nerve," *J. Amer. Soc. Surg. Hand*, vol. 4, no. 3, pp. 227–230, 2004.

[26] R. J. Schultz, J. Furlong, and A. Storace, "Detailed anatomy of the extensor mechanism at the proximal aspect of the finger," *J. Hand Surg. Amer.*, vol. 6, no. 5, pp. 493–498, 1981.

[27] J. R. Doyle, "Anatomy of the finger flexor tendon sheath and pulley system," *J. Hand Surg. Amer.*, vol. 13A, no. 4, pp. 473–484, 1988.

[28] R. A. Chase and W. L. White, "Functional anatomy of the hand," Stanford Anatomy. [Online]. Available: https://www.youtube.com/watch?v=9V1ZzAiB1rY&t=1504s